BIOCELL

Tech Science Press

Doi:10.32604/biocell.2025.063296

ARTICLE

CLDN9 Levels Influence the Biological Activities of Cells in Gastric Cancer

Jin Liu[1,2], Xiu Zhang[1], Xiao Hu[2], Gaofeng Yuan[2] and Kai Chen[1,*]

[1]Department of Oncology, The First Affiliated Hospital of Soochow University, Suzhou, 215000, China
[2]Department of Oncology, Suqian First Hospital, Suqian, 223800, China

*Corresponding Author: Kai Chen. Email: cky9920@163.com

Received: 10 January 2025; Accepted: 08 April 2025; Published: 30 April 2025

ABSTRACT: Objective: This study examines the significance and functions of CLDN9 in gastric cancer (GC), intending to identify novel targets for diagnosis and treatment. **Methods:** CLDN9 expression in GC tissues and cell lines was investigated in TCGA data, with analysis with Western blotting, qRT-PCR, and immunohistochemical analyses. Correlations between clinicopathological characteristics, progression-free survival (PFS), and overall survival (OS) were assessed with Cox regression. The effect of CLDN9 knockdown/overexpression on tumorigenic functions (proliferation, migration, and invasion) was assessed using CCK-8, colony formation, and Transwell assays. Tumor-bearing assays were performed to verify the impact of CLDN9 knockdown on the *in vivo* proliferation of GC cells. **Results:** Analysis of TCGA data, qRT-PCR, Western blotting, and immunohistochemistry indicated significantly elevated levels of CLDN9 in GC tissues and cell lines ($p < 0.01$). Compared to the group with high CLDN9 expression, PFS and OS were markedly longer in cases with low CLDN9 levels ($p < 0.05$). Multivariate regression indicated that CLDN9 levels were independently predictive of GC prognosis. CCK-8, Transwell, and colony formation tests showed that CLDN9 overexpression promoted GC cell proliferation, clonogenicity, and migratory/invasive capabilities, but CLDN9 knockdown markedly reduced these features. Experiments involving tumor-bearing models demonstrated that the suppression of CLDN9 inhibited the *in vivo* growth of GC cells. **Conclusion:** In conclusion, this study's findings suggested that CLDN9 might be a valuable therapeutic target or diagnostic biomarker for GC.

KEYWORDS: Gastric cancer; CLDN9; cell proliferation; invasion; migration

1 Introduction

Among the primary causes of global cancer-associated deaths, gastric cancer (GC) ranks 3rd in worldwide cancer-related mortality. According to World Health Organisation (WHO) statistics, stomach cancer follows lung cancer and colorectal cancer [1–4]. In areas with higher GC incidence, especially in East and Southeast Asia, rates remain high and demonstrate an increasing trend among younger demographics. The prevalence of GC is increasing, attributed to lifestyle modifications, imbalanced dietary habits, and environmental influences, including *Helicobacter pylori* infection [5]. However, many individuals receive diagnoses at advanced stages, resulting in suboptimal treatment outcomes and adverse prognoses [6–8]. Many patients have missed the most effective opportunity for therapy upon diagnosis due to a lack of customized treatment options and ineffective early diagnostic biomarkers [9,10], despite advancements in diagnostic technology and therapeutic approaches over the previous few decades [11]. The high recurrence rate and low survival rate of GC pose significant challenges to its treatment [12]. Therefore, exploring new molecular markers for GC and their potential mechanisms has become an essential focus of current research [13,14] to provide new approaches for early screening and targeted therapy.

Copyright © 2025 The Authors. Published by Tech Science Press.
This work is licensed under a Creative Commons Attribution 4.0 International License, which permits unrestricted use, distribution, and reproduction in any medium, provided the original work is properly cited.

Claudin 9 (CLDN9) is crucial for cell-cell adhesion [15,16]. The abnormal expression of CLDN9 can lead to altered cell-cell interactions, increased permeability, and tumorigenesis [17,18]. For example, abnormal expression of CLDN9 in endometrial carcinoma is linked with poor outcome [19] while high CLDN9 levels in pituitary adenomas are associated with metastasis [20]. According to Hu et al. [21], CLDN9 suppresses $CD8^+$ T cell anti-tumor functions while promoting glycolysis and lactylation of PD-L1, advancing GC progression.

Here, the pathophysiological and prognostic consequences of claudin-9 transcriptome expression were investigated in patients with GC. By examining CLDN9's function in GC, we intend to establish novel molecular targets and theoretical frameworks for early detection, targeted therapy, and the formulation of personalized treatment approaches for GC.

2 Study Methodology

2.1 Cell Culture

The ATCC cell bank provided the human GC cell lines AGS, MGC-803, HGC-27, and the normal gastric mucosal epithelial cell line GES-1. Cells were cultured in RPMI 1640 medium (Gibco, Catalog No. R8758, Waltham, MA, USA) supplemented with 10% fetal bovine serum (FBS, Thermo Fisher, Catalog No. 12103C, Waltham, MA, USA), penicillin (100 IU/mL, Sigma-Aldrich, Catalog No. P0389, St. Louis, MO, USA), and streptomycin (100 µg/mL, Sigma-Aldrich, Catalog No. S9137). All cell lines were maintained at 37°C in a humidified atmosphere containing 5% CO_2. To ensure the validity of experimental results, all cell lines were routinely tested for mycoplasma contamination using a PCR-based detection kit (Takara Bio Inc., Catalog No. 6601, Shiga, Japan), and only mycoplasma-free cells were used in subsequent experiments.

2.2 TCGA Data

The TCGA (http://cancergenome.nih.gov/, accessed on 01 April 2025) database was used for publicly available data to analyze CLDN9 expression levels in GC tissues. There were 624 samples, of which 414 were cancerous and 210 normal.

2.3 Clinical Tissue and Pathological Data Collection

GC patients who had surgery at Suqian First People's Hospital between January 2016 and December 2018 had clinical tissue samples and pathological information gathered from them. Seventy-six identical samples of the surrounding non-tumor tissues (N) and primary tumor tissues (T) of GC were gathered. The GC tissue samples were immunohistochemically stained and analyzed for survival. All clinical sample utilization received approval from the Suqian First People's Hospital Ethics Committee (No. 20230026) and complied with the principles of the Declaration of Helsinki (1964). Written informed consent was obtained from all participants before sample collection.

2.4 Immunohistochemical Staining

Tumor tissue samples were fixed, embedded in paraffin, and sectioned into 2 µm slices. Sections were deparaffinized in xylene and rehydrated through a graded ethanol series (100%, 90%, and 70%) followed by PBS washes. After antigen retrieval in citrate buffer (pH 6.0) at 95°C for 20 mins, the slides were cooled to room temperature. To permeabilize cell membranes, sections were incubated in 0.2% Triton X-100 (Aladdin, Catalog No. T743333, Shanghai, China) for 10 mins. Endogenous peroxidase activity was blocked by incubation in 3% hydrogen peroxide for 10 mins at room temperature. Nonspecific binding was blocked using 5% bovine serum albumin (BSA, Sigma-Aldrich, Catalog No. A9418, Louis, MO, USA) in PBS for 30 min. The sections were then incubated overnight at 4°C with polyclonal antibodies against CLDN9

(1:100, Abcam, ab245235, Cambridge, UK) or Ki-67 (1:150, Abcam, ab15580). Following rinsing with PBS, the sections were treated with a biotinylated secondary antibody (anti-rabbit IgG, 1:500, Abcam, ab6721) for 30 mins at room temperature, followed by treatment with DAB (Vector Laboratories, Catalog No. SK-4100, Newark, CA, USA). Following staining, a light microscope (Leica DM3000, Germany) was utilized for imaging. The staining intensity and the quantity of positive cells determined the score. With scores of 0, 1, 2, 3, and 4, the positive cell proportion was categorized as follows: less than 10%, 10%–25%, 26%–50%, 51%–75%, and >75%. Staining intensities were classified as: light yellow (scoring 1), brown-yellow (score 2), brown (score 3), and no color (score 0). The product of the positive cell counts and the staining intensity determined the final score. A score of ≤4 characterizes CLDN9 low expression, while CLDN9 high expression is indicated by a score of >4.

2.5 The qRT-PCR Assay

Approximately 50 mg of tumor tissue or 1×10^5 GC cells were homogenized in TRIzol reagent (Invitrogen (Thermo Fisher Scientific), Catalog No. 15596026, Waltham, MA, USA) on ice. Following centrifugation, the supernatant was obtained, and total RNA was extracted using the Total RNA Extraction Kit (Invitrogen (Thermo Fisher Scientific), Catalog No. 12183025) as per recommendations. The RNA underwent reverse transcription into cDNA, employing the RNA Reverse Transcription Kit (RR047A, Takara, Japan). GAPDH served as an internal control, and cDNA was quantified employing SYBR Green reagent (RR820A, Takara, Japan). The primer sequences (human species) used were:

Forward-CLDN9: 5′-TTTCTCCAGTGAATCCCGGA-3′

Reverse-CLDN9: 5′-AAGGGAAGTGGCATTTGCC-3′

Forward-GAPDH: 5′-GGEGGCACTGTGATCCTAC-3′

Reverse-GAPDH: 5′-TCGGEGAGTGTGGATGAGG-3′

2.6 Western Blotting

A protease inhibitor cocktail (Roche Diagnostics GmbH, Catalog No. 04693159001, Baden-Württemberg, Germany) was added to 100 μL of lysis solution, and about 100 mg of tumor tissue was homogenized on ice for two mins before being lysed for 20 min. As an alternative, 100 μL of the same lysis buffer was used to lyse around 2×10^6 GC cells for 20 min on ice. Protein content was ascertained using Pierce Chemical's BCA Assay Kit (Thermo Fisher Scientific, Catalog No. 23225, Waltham, MA, USA). SDS-PAGE separated 30 μg of total protein, which were then deposited onto PVDF membranes (Merck Millipore, Catalog No. IPVH00010, Hessen, Germany), which were blocked for two hours with 5% BSA (Sigma-Aldrich, Catalog No. A9418). Rabbit anti-human CLDN9 (Abcam, ab245235) and β-actin (Abcam, ab8226) antibodies (1:1000) were then incubated for the entire night at 4°C. After washing, the membranes were incubated with HRP-conjugated secondary antibodies (1:5000, Santa Cruz Biotechnology, Catalog No. sc-2004, Dallas, TX, USA) at room temperature for 1.5 h, with visualization with an ECL system (Thermo Fisher [iBright series], Catalog No. CL1500).

2.7 Synthesis of Vector and Cellular Transfection

A short hairpin RNA (shRNA) lentiviral vector that targeted the CLDN9 gene was created using the pSilencer 2.1-U6 puro vector (Thermo Fisher) and transfected into HGC27 cells. After transfection, puromycin (Thermo Fisher) was selected to isolate stable HGC27 cells with CLDN9 knockdown. The following shRNA sequences were used: shR1: 5′-CCAAGTTGTG-AATGTTGTACAGA-3′; shR2: 5′-TGAGGTAGC-ACCACGTACTG-3′; shCtrl: 5′-GTCTCCCG-AACCTCACGT-3′. To overexpress the CLDN9 gene, an

expression vector containing the full-length CLDN9 gene was constructed. After being cloned into the pCMV-Tag 2B vector (Agilent Technologies, Santa Clara, CA, USA) and amplified by PCR, the CLDN9 gene was transfected into AGS cells. Following transfection, stable AGS cells with CLDN9 overexpression were obtained using G418 (Thermo Fisher) selection.

2.8 Cell Proliferation Assay

CCK-8 assays (Beyotime, C0038, Shanghai, China) were utilized to assess proliferation. Three thousand GC cells/well were inoculated in 96-well plates. After 12 h of incubation, 10 μL of CCK-8 reagent were added for 2 h at 37°C, followed by measuring absorbances at 450 nm in a Multiskan SkyHigh microplate reader (Thermo Fisher) [22].

2.9 Colony Formation Assays

After being gathered, 1000 GC cells were sown into each 6-well plate. After two weeks of culture, the colonies were rinsed with PBS, fixed with 4% paraformaldehyde, and stained with crystal violet for 30 min away from light. Following a PBS wash to eliminate any remaining crystal violet, the colonies were enumerated under optical microscopy (Olympus, Catalog No. CKX53, Tokyo, Japan).

2.10 Transwell Assay

For 12 h, GC cells were kept in RPMI-1640 media without FBS. A Transwell insert's upper chamber was filled with Matrigel (BIOSCIENCES, Catalog No. 354234, Woburn, MA, USA) and an equivalent volume of RPMI-1640 media. The upper compartment was seeded with stomach cancer cells once the Matrigel had solidified. For 48 h, the Transwell inserts were incubated at 37°C in a 12-well plate filled with RPMI-1640 medium. Paraformaldehyde was used to fix the cells that had been transferred to the bottom compartment, and they were then stained with crystal violet for half an hour in the dark. Cells were enumerated under optical microscopy (Olympus, CKX53).

2.11 Nude Mouse Xenograft Experiment

Male BALB/c nude mice (4–8 weeks) were purchased from Shanghai Laboratory Animal Center, Chinese Academy of Sciences (China). The average body weight of the mice was between 18–22 g at the time of the experiment. Mice were kept at 22 ± 2°C, with relative humidity of 50 ± 10%, and a 12-h light/dark cycle, with unrestricted sterilized rodent chow and tap water. The animals were acclimated for a minimum of 1 week before experiments. Six mice each were randomly assigned to a CLDN9 knockdown and control group, and 5×10^6 CLDN9 knockdown or wild-type HGC-27 cells were administered subcutaneously into the left flanks of the mice. Calipers were used to measure the tumor volume once a week for four weeks, after which the animals were sacrificed, and the tumors were collected and weighed. Immunohistochemical staining was used to determine whether the tumor tissues expressed CLDN9 and Ki-67. The Soochow University Ethics Committee approved all animal studies (Approval No. SUDA20240711A09). All animal experiments were performed in accordance with a protocol approved by the Institutional Animal Care and Use Committee of Soochow University.

2.12 Statistical Analysis

The analysis was conducted using IBM SPSS 26.0 (IBM Corporation, New York, NY, USA). The mean ± standard error (SD) represents the results. Two groups were compared using *t*-test, and multiple groups using one-way analysis of variance (ANOVA). Spearman's rank correlations were utilized to assess associations.

Kaplan-Meier curves and log-rank tests were used to conduct survival analysis. Each experiment had a sample size of three. Statistical significance is represented by $p < 0.05$.

3 Results

3.1 CLDN9 Levels Are Elevated in GC Cells and Tissues

Data from the TCGA indicated that CLDN9 levels were markedly elevated in GC tissues relative to normal and adjacent non-cancerous tissues (Fig. 1A,B). Thirty GC samples and their paired neighboring tumor tissues were subjected to qRT-PCR to verify CLDN9 levels in GC. The findings demonstrated that compared to nearby non-cancerous cells, GC tissues had much greater CLDN9 expression (Fig. 1C). At the cellular level, GC cell lines showed considerably higher levels of CLDN9 expression than normal gastric epithelial cells (GES-1), shown by qRT-PCR and Western blotting (Fig. 1D,E). CLDN9 expression was significantly elevated in the cytosol and cell membranes of GC cells, with a higher positive score than normal tissues, according to an immunohistochemical study of lesion tissues from 76 individuals with GC (Fig. 1F). These findings indicate that CLDN9 expression is elevated in GC samples and cells, pointing to a possible involvement of CLDN9 in GC pathology and bolstering its application as a biomarker for GC diagnosis or prognosis.

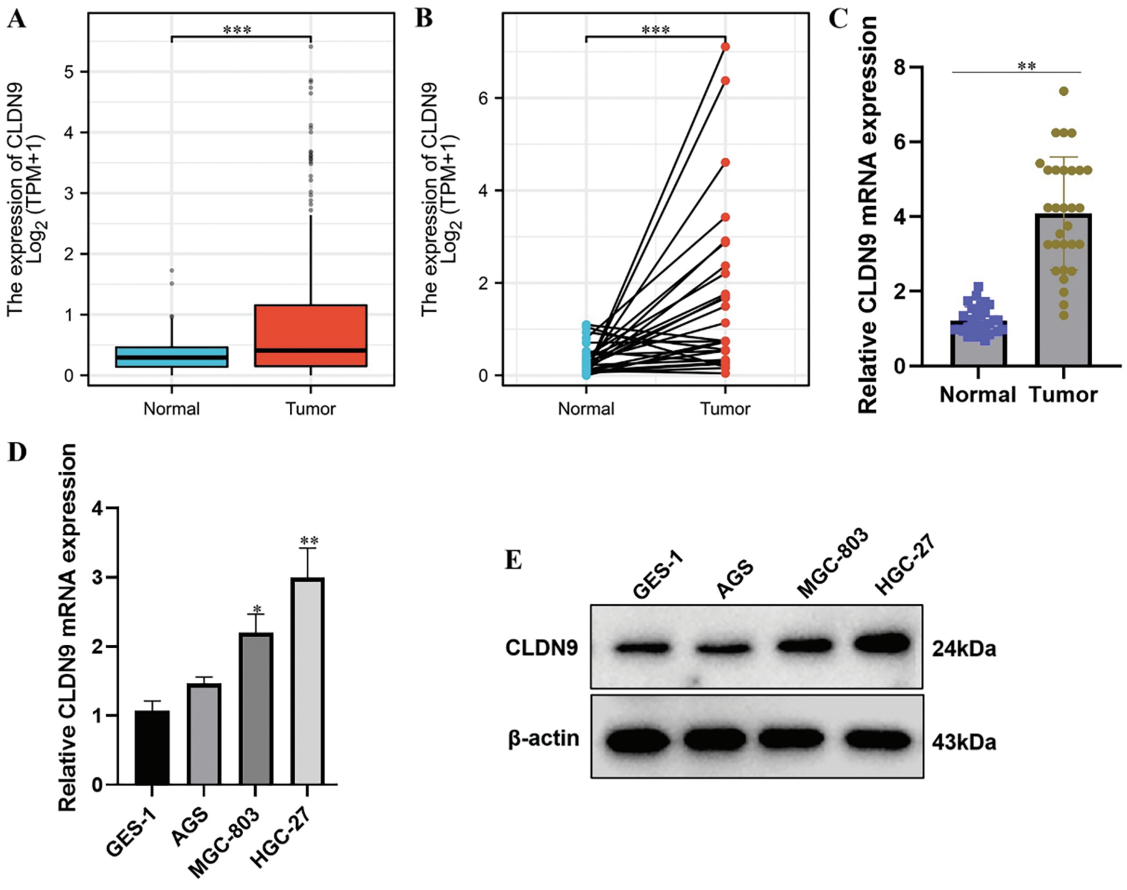

Figure 1: (Continued)

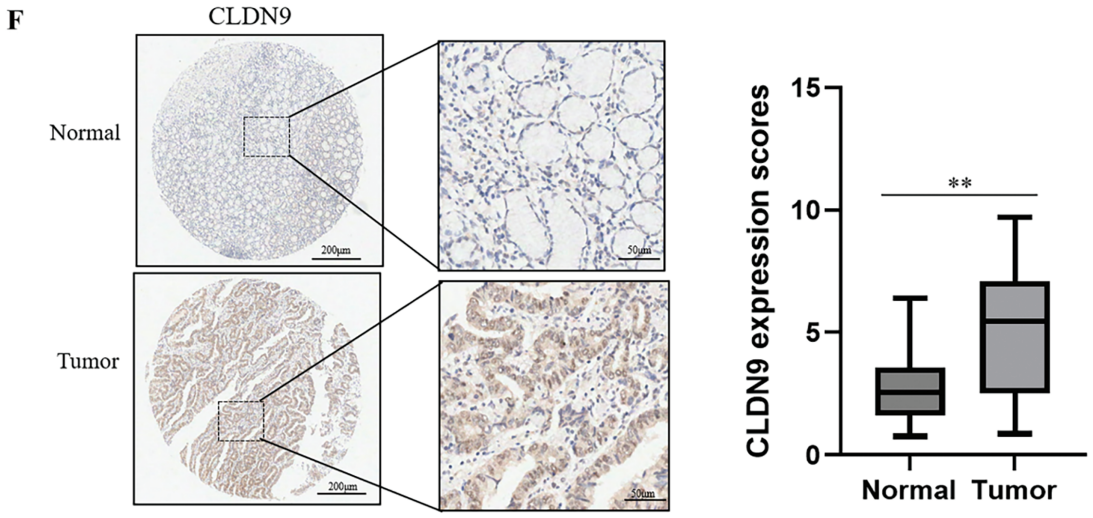

Figure 1: CLDN9 levels are elevated in GC cell lines and tissues. (**A**) CLDN9 levels in normal gastric and GC samples, from the TCGA. (**B**) CLDN9 levels in 27 paired GC and normal tissues. (**C**) qRT-PCR detection of CLDN9 in 30 GC and normal tissues. (**D,E**) CLDN9 levels in GC cell lines (AGS, HGC-27, and MGC-803), shown by qRT-PCR and Western blotting. (**F**) CLDN9 levels in GC tissues and normal tissues, shown by immunohistochemistry (*$p < 0.05$; **$p < 0.01$; ***$p < 0.001$)

3.2 Associations between CLDN9 Levels and Clinical Parameters

To evaluate the clinical importance of CLDN9 levels in GC, a correlation analysis between CLDN9 expression and clinical pathological features was performed. Twenty-eight patients were allocated to the low-CLDN9 group, while forty-eight patients were assigned to the high-CLDN9 group. CLCN9 levels were found to be markedly connected ($p < 0.05$) to tumor diameter, lymph node metastasis, and TNM stage. Patients who expressed CLDN9 had larger tumor diameters, more lymph node metastases, and more advanced TNM stages (III–IV) (Table 1).

Table 1: Relationship examination of CLDN9 expression with clinical characteristics in GC patients

Clinical features	Total (n = 76)	CLDN9 lower expression group (n = 28)	CLDN9 higher expression group (n = 48)	χ^2	p
Sex				0.1822	0.6695
Male	41	16	25		
Female	35	12	23		
Age				0.0157	0.9003
≤60	40	15	25		
>60	36	13	23		
Tumor diameter				4.463	0.0346
≤5 cm	29	15	14		
>5 cm	47	13	34		
Degree of differentiation				2.114	0.1460

(Continued)

Table 1 (continued)

Clinical features	Total (n = 76)	CLDN9 lower expression group (n = 28)	CLDN9 higher expression group (n = 48)	χ^2	*p*
Poor	24	6	18		
Moderate-high	52	22	30		
Lauren classification				1.668	0.1965
Intestinal type	59	24	35		
Diffuse type	17	4	13		
Lymph node metastasis				5.876	0.0153
Yes	51	14	37		
No	25	14	11		
TNM staging				6.303	0.0121
I–II	27	15	12		
III–IV	49	13	36		
Vascular invasion				0.1122	0.7377
Yes	29	10	19		
No	47	18	29		
Nerve invasion				3.836	0.0502
Yes	35	17	18		
No	41	11	30		

Note: $p < 0.05$ indicates statistical significance.

3.3 CLDN9 Expression and Its Association with Prognosis in GC Patients

A survival analysis using the TCGA database showed that GC cases with high CLDN9 levels had markedly lower DSS, OS, and PFS than those with low CLDN9 (Fig. 2A). The CLDN9 low-expression group had substantially better compared PFS and OS than the high-expression group, according to our analysis of survival data from 76 patients (PFS: 54.75 ± 2.00 vs. 44.47 ± 1.67 months, $p = 0.023$; OS: 59.43 ± 0.80 vs. 56.18 ± 1.15 months, $p = 0.047$) (Fig. 2B).

3.4 Univariate and Multivariate Analyses of Prognostic Factors

CLDN9 expression, Lauren classification, TNM stage, and neural invasion were independently predictive of GC prognosis, according to the findings of the univariate and multivariate analyses (Table 2).

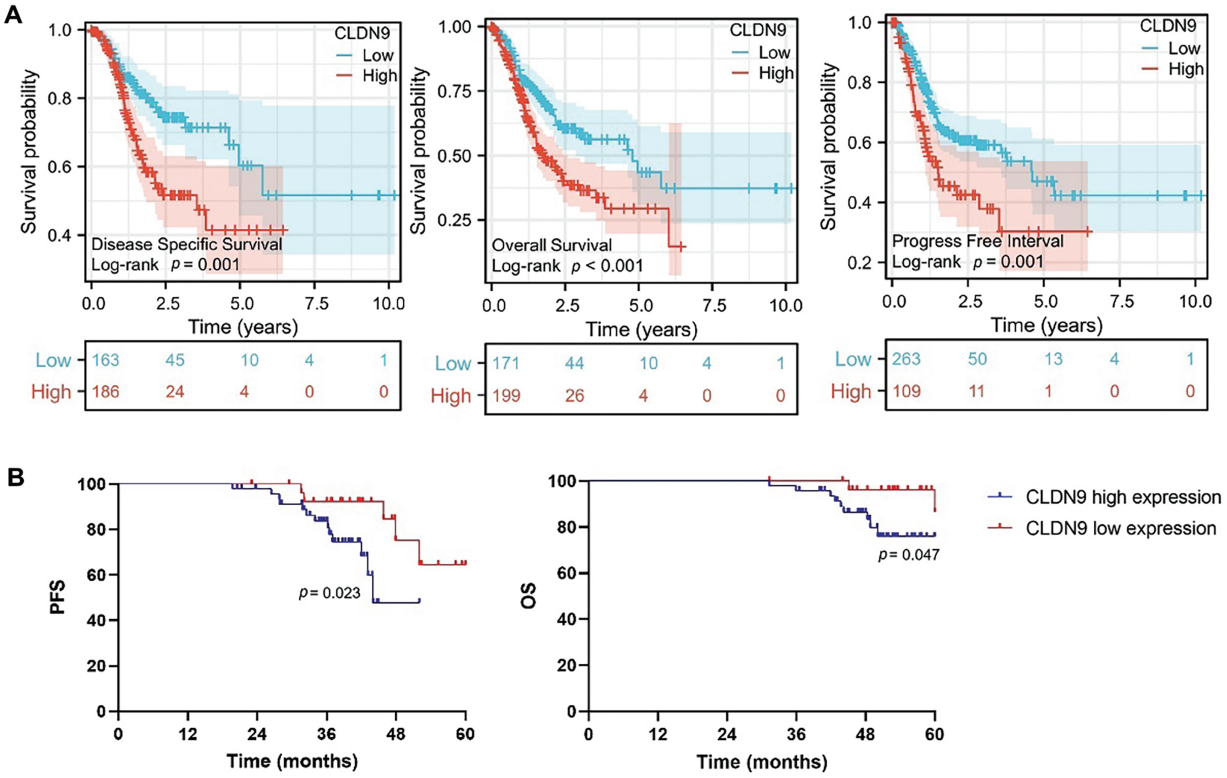

Figure 2: GC patients' prognosis and CLDN9 expression. (**A**) CLDN9 expression levels and Disease-Specific Survival (DSS), Overall Survival (OS), and Progression-Free Survival (PFS) in GC patients were analyzed using the TCGA database. (**B**) PFS and OS comparison in 76 GC cases with varying CLDN9 levels

Table 2: Cox univariate and multivariate analysis of prognostic factors in GC

Clinical features	*p*-value	Exp(B)	95.0% CI of Exp(B)		*p*-value	Exp(B)	95.0% CI of Exp(B)	
			Lower limit	Upper limit			Lower limit	Upper limit
CLDN9 expression	0.003	18.637	2.666	130.29	0.001	12.01	2.732	52.84
Sex	0.807	1.154	0.367	3.629	–	–	–	–
Age	0.211	2.144	0.649	7.079	–	–	–	–
Tumor diameter	0.308	2.475	0.433	14.14	–	–	–	–
Degree of differentiation	0.184	2.15	0.695	6.649	–	–	–	–
Lauren classification	0.006	8.818	1.841	42.24	0.001	11.72	2.609	52.64
Lymph node metastasis	0.912	1.168	0.074	18.42	–	–	–	–
TNM staging	0.011	20.103	1.997	202.38	0.001	24.38	3.882	153.12
Vascular invasion	0.868	1.124	0.283	4.467	–	–	–	–
Nerve invasion	0.028	6.785	1.236	37.26	0.026	6.479	1.255	33.44

3.5 Construction of CLDN9 Knockdown/Overexpression GC Cell Lines

Western blotting and qRT-PCR confirmed the successful overexpression and knockdown of CLDN9 in GC cells. In HGC-27 cells, lentiviral vectors shR1 and shR2 significantly decreased CLDN9's mRNA and protein levels (Fig. 3A). Further, CLDN9 was successfully overexpressed in AGS cells using the CLDN9 overexpression vector at both the mRNA and protein levels (Fig. 3B).

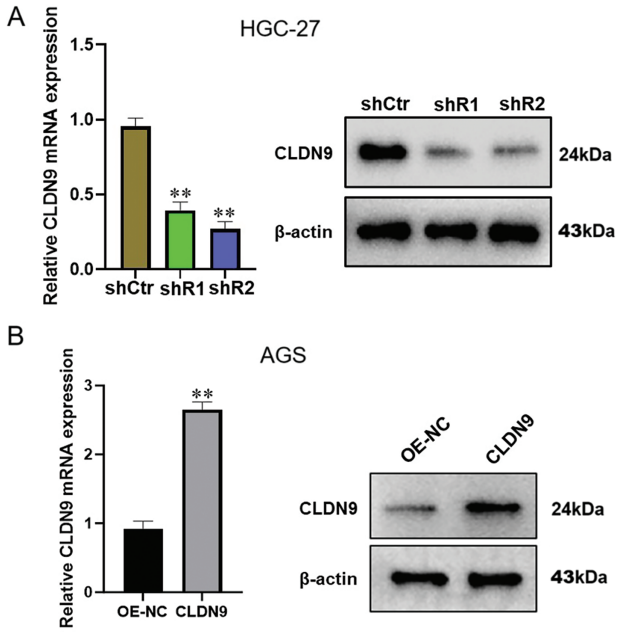

Figure 3: CLDN9 levels in GC cell lines with knockdown/overexpression. (**A**) Following transfection with lentiviral vectors shR1 and shR2, the levels of CLDN9 in HGC-27 cells were assessed by Western blotting and qRT-PCR. (**B**) qRT-PCR and Western blotting analyzed the levels of CLDN9 in AGS cells after transfection with the overexpression vector (**$p < 0.01$)

3.6 Effects of Overexpression/Knockdown CLDN9 on GC Cell Proliferation and Clonogenicity

According to CCK-8 data, HGC-27 cell proliferation was significantly decreased by CLDN9 knockdown (shR1 and shR2 groups) (Fig. 4A), whereas AGS cell proliferation was enhanced considerably by CLDN9 overexpression (Fig. 4B). Similarly, CLDN9 overexpression significantly enhanced the clonogenic potential of AGS cells (Fig. 4D), whereas CLDN9 knockdown (shR1 and shR2 groups) substantially reduced the clonogenic potential of HGC-27 cells (Fig. 4C).

3.7 Effects of CLDN9 Overexpression and Knockdown on GC Cell Migration and Invasion

Transwell tests showed that CLDN9 overexpression significantly raised GC cell migration and invasion capabilities (Fig. 5B), but CLDN9 knockdown significantly reduced these abilities (Fig. 5A).

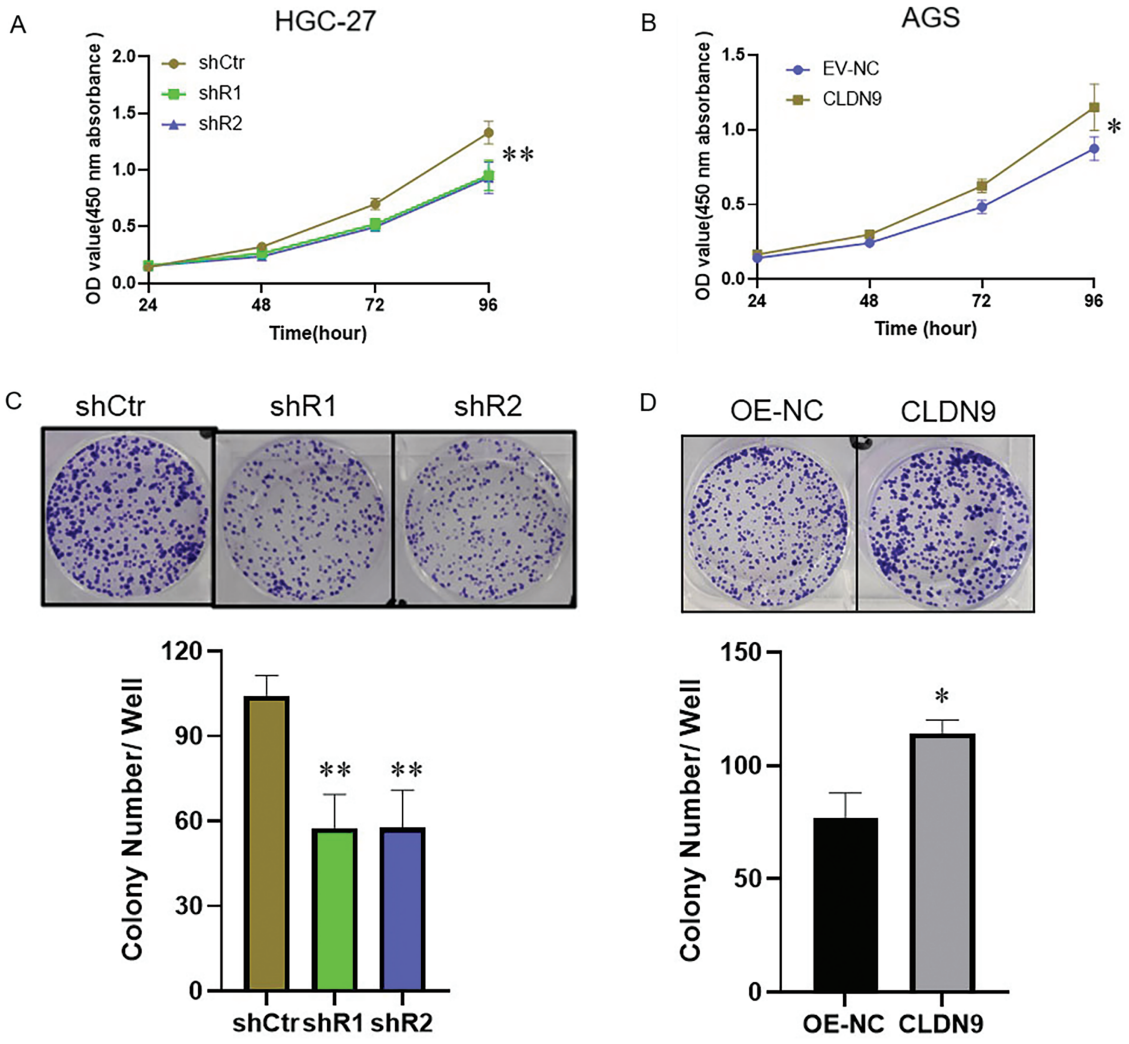

Figure 4: CLDN9 knockdown/overexpression effect on GC cell proliferation and clonogenicity. CCK-8 assays showed that (**A**) substantially decreased GC cell proliferation, whereas (**B**) significantly enhanced GC cell proliferation. CLDN9 knockdown dramatically reduced the number of colonies produced from GC cells (**C**). However, clonogenic experiments showed that CLDN9 overexpression (**D**) substantially enhanced the GC cells' capacity to proliferate (*$p < 0.05$, **$p < 0.01$)

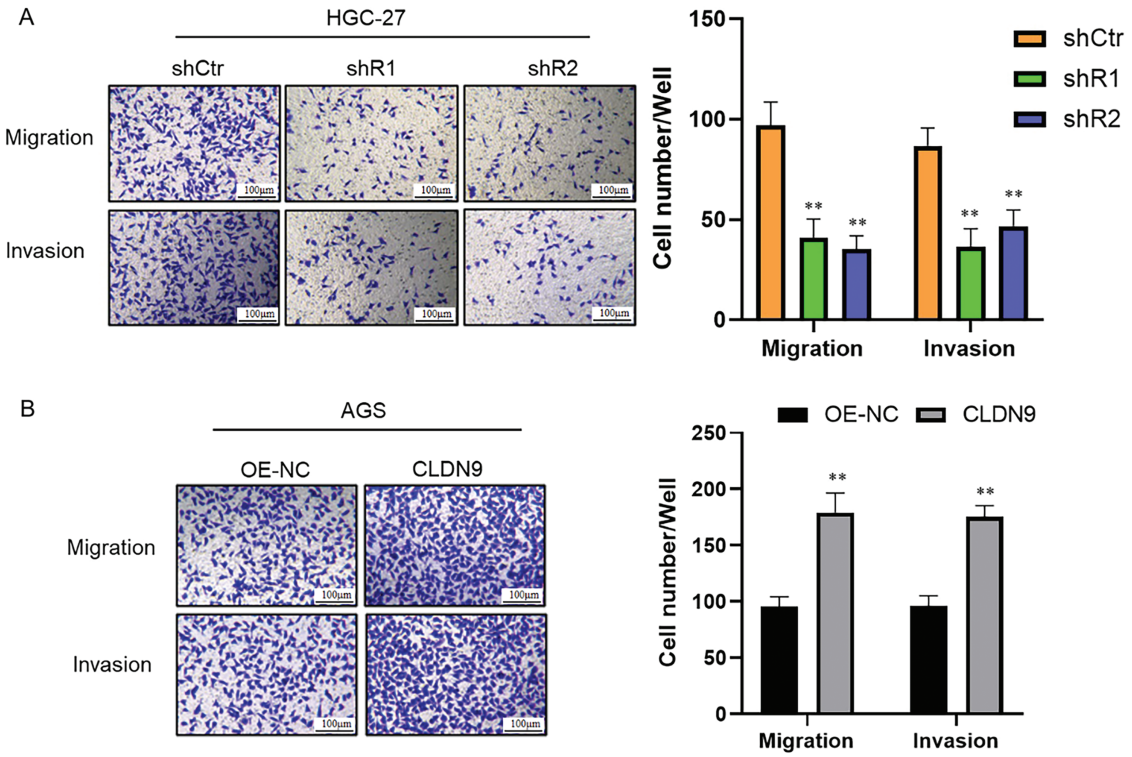

Figure 5: GC cell migration and invasion affected by CLDN9 overexpression and knockdown. Using Transwell assays, the effects of CLDN9 knockdown on the migratory and invasion capabilities of HGC-27 (**A**) and AGS (**B**) cells were investigated (**$p < 0.01$)

3.8 CLDN9 Knockdown's Impact on GC Cell Proliferation In Vivo

We performed a xenograft experiment using nude mice to verify whether CLDN9 similarly regulates tumor growth *in vivo*. HGC-27 cells with stable CLDN9 knockdown (shR1 and shR2 groups) and control group (shCtrl) were injected subcutaneously into the mouse flanks. *In vivo* data demonstrated that relative to the blank control (shCtr), the tumor width, volume, and weight in the shR1 and shR2 groups decreased substantially (Fig. 6A–C), showing that the growth of GC cells in nude mice was suppressed. qRT-PCR analysis indicated that CLDN9 mRNA levels in tumor tissues from the shR1 and shR2 groups were substantially decreased relative to the blank control sequence (shCtr) (Fig. 6D).

3.9 Immunohistochemical Analysis of CLDN9 and Proliferation Marker Ki-67 Expression in Tumor Tissues

Immunohistochemical staining of xenograft tumor tissues was performed. The findings demonstrated that CLDN9, which was primarily found in the cell membrane and cytoplasm, had a higher positive staining ratio in the blank control group (shCtr). In contrast, CLDN9 staining in the knockdown groups (shR1 and shR2) was significantly weaker (Fig. 7). Further detection of the cell proliferation marker Ki-67 revealed that the staining intensity for Ki-67 was higher in the control group (shCtr), with a more significant proportion of positive cells. In contrast, the knockdown groups (shR1 and shR2) showed weaker Ki-67 staining with a lower percentage of positive cells. The results suggest that CLDN9 overexpression stimulates GC cell proliferation *in vivo* (Fig. 7).

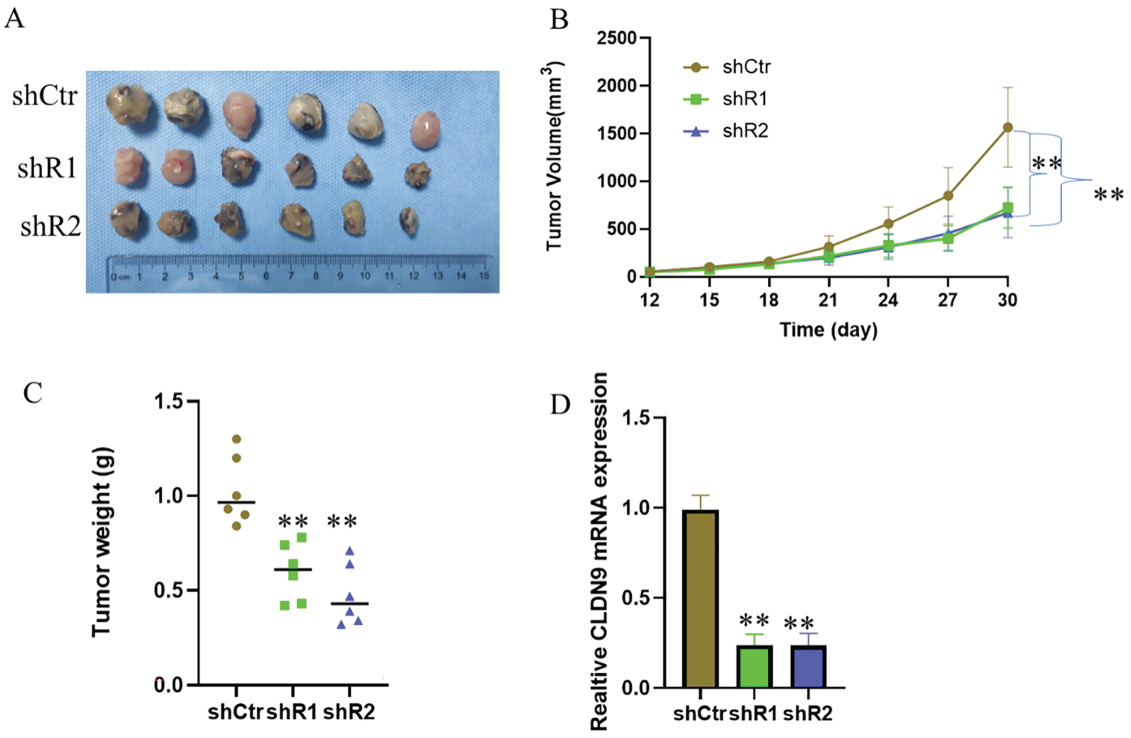

Figure 6: Effects of CLDN9 knockdown on GC tumor growth *in vivo*. (**A**) Tumors after 30 days of growth. (**B**) Tumor volume measurement starts 12 days after subcutaneous injection, with the growth curve plotted. (**C**) Analysis of tumor tissue weight. (**D**) The qRT-PCR analysis of CLDN9 mRNA levels in tumor tissues from different groups (**$p < 0.01$)

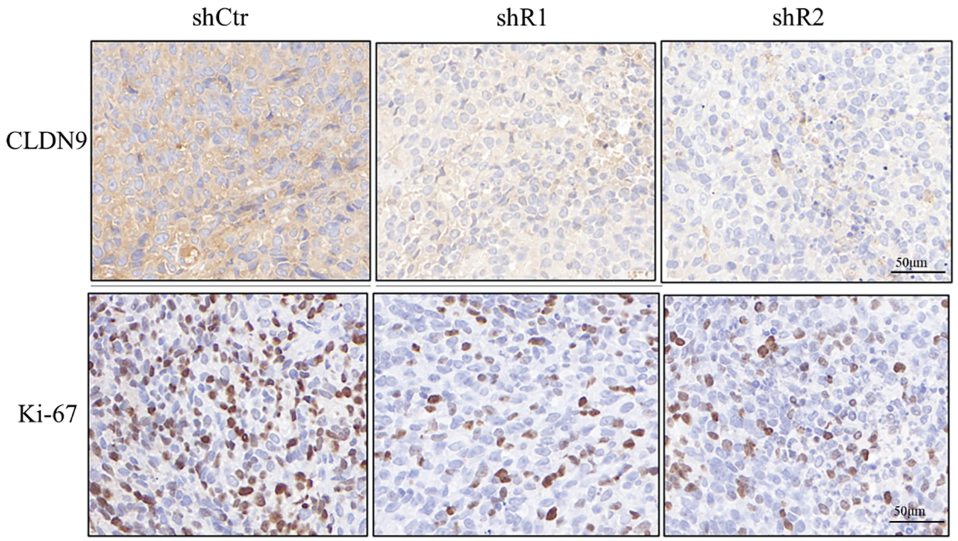

Figure 7: (Continued)

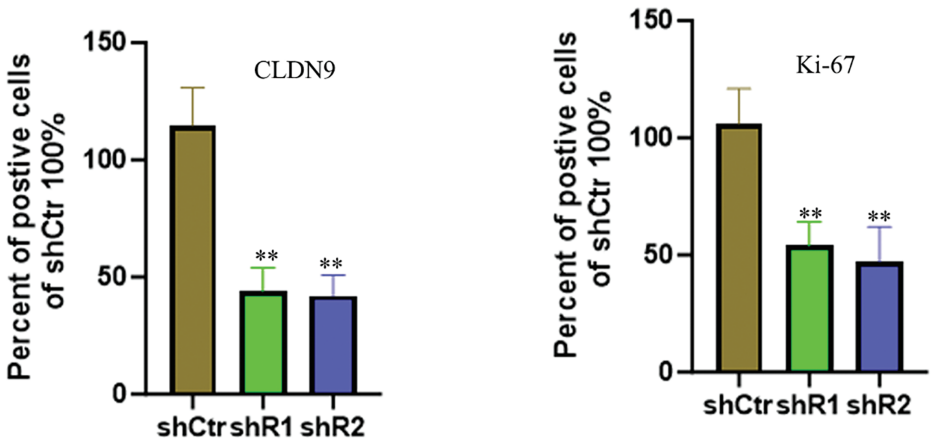

Figure 7: Immunohistochemical analysis of CLDN9 and proliferation-related nuclear antigen Ki-67 expression in tumor-bearing tissues (**$p < 0.01$)

4 Discussion

Claudins (CLDN) are a group of structural proteins that help cells adhere together. They are essential for maintaining the adhesion between stomach epithelial cells, allowing specific molecules to pass through the epithelial cell layer, and maintaining the balance of ions in the stomach [23,24]. The clinical importance and possible use of CLDN proteins in the prognosis, diagnosis, and treatment of GC have been shown in recent investigations [25,26]. For example, the loss or downregulation of CLDN-3, 4, and 18 in gastric mucosa suggests the presence of precancerous and early-stage lesions [26,27]. In GC, the downregulation of CLDN-3, 4, and 18 is associated with increased tumor diameter, deeper invasion, or more extensive lymphatic spread, all of which indicate greater malignancy and are closely correlated with later-stage disease and poor prognosis [28–30]. The invasion and metastasis of epithelial-derived tumors, such as GC, are often associated with abnormalities in tight junction function. The downregulation of CLDN proteins is considered one of the key factors driving tumor invasion and metastasis [31]. However, this study is the first to demonstrate the overexpression of CLDN9 in GC tissues and its substantial influence on the biological functions of GC cells, in contrast to the expression patterns of CLDN-3, 4, and 18. This suggests that CLDN9 may play an integral part and mechanism in GC development that deviates from earlier understandings of CLDN biological functions.

Using qRT-PCR and TCGA database analysis, this study first demonstrated that CLDN9 levels are elevated in both GC tissues and cell lines relative to normal gastric epithelia. The high levels of CLDN9 in the cell membranes and cytoplasm of GC tissues were further confirmed by immunohistochemical investigation. These results provide validity to CLDN9's possible involvement in the development and progression of GC. Evaluation of clinical pathological parameters indicated significant associations between increased CLDN9 expression and TNM staging, tumor diameter, and lymph node metastases in GC patients. Larger tumors, lymph node metastases, and advanced TNM stages are linked to high CLDN9 expression in patients, indicating that it may be used as a marker of GC prognosis. Survival analysis revealed that patients exhibiting high CLDN9 expression experienced significantly reduced DSS, OS, and PFS than those with low expression levels. Cox multivariate analysis further demonstrated the strong correlation between CLDN9 and a poor prognosis by confirming that elevated CLDN9 levels are independently predictive of GC prognosis.

In terms of cellular functional experiments, we constructed GC cell lines with CLDN9 knockdown and overexpression to investigate the effects of CLDN9 on GC cell proliferation, colony formation, invasion, and

migration. CLDN9 knockdown substantially enhanced the ability of GC cells to invade and migrate, as well as their ability to proliferate and form colonies. On the other hand, CLDN9 overexpression greatly enhanced these biological processes. The results indicate that CLDN9 may improve the course of GC malignancy by modulating GC cells' proliferation and metastatic capabilities. Furthermore, *in vivo* investigations corroborated the CLDN9 involvement in GC cell proliferation.

Currently, the biological functions of CLDN9 are primarily understood in the context of epithelial and epidermal permeability, barrier protection, and cell junctions [16]. However, recent studies have shown that in other cancers, the upregulation of CLDN9 enhances the motility and invasiveness of tumor cells. For example, CLDN9 upregulation in hepatocellular carcinoma promotes tumor cell invasion by activating the Tyk2-Stat3 pathway [32]. At the same time, CLDN9 knockdown in lung cancer effectively decreases cell motility, *in vitro* invasiveness, and *in vivo* metastasis [33]. It also significantly inhibits the epithelial-to-mesenchymal transition (EMT) process in colorectal cancer CT26 cells [34]. Moreover, CLDN9 may act as a glycolytic regulatory factor in energy metabolism regulation in endometrial carcinoma, potentially influencing cell proliferation [35]. These studies indicate that CLDN9 plays multiple regulatory roles in tumor development and has unique potential as a cancer therapy target. However, more research is required to clarify the precise functions of CLDN9 as an effective treatment in GC.

This study demonstrates that CLDN9 is strongly linked to a bad prognosis for GC patients and is markedly elevated in GC cells. Overexpression of CLDN9 significantly promotes GC growth and metastatic ability in cellular models. The findings of this work present a new possible therapeutic target and diagnostic biomarker for GC, therefore offering a preliminary understanding of the function of CLDN9 in GC formation.

Acknowledgement: Not applicable.

Funding Statement: This study was supported by the Science and Technology Plan of Suqian City (Grant No. S202117).

Author Contributions: Study design and concept: Jin Liu and Kai Chen. Data acquisition: Jin Liu, Xiu Zhang, and Gaofeng Yuan. Data analysis and interpretation: Xiao Hu and Kai Chen. Manuscript preparation: Kai Chen. Manuscript review: Jin Liu and Xiao Hu. All authors contributed to editorial changes in the manuscript. All authors have participated sufficiently in the work and agreed to be accountable for all aspects of the work. All authors reviewed the results and approved the final version of the manuscript.

Availability of Data and Materials: The datasets used and analyzed during the current study are available from the corresponding author upon reasonable request.

Ethics Approval: All clinical sample usage was approved by the Suqian First Hospital Ethics Committee (No. 20230026) and adhered to the principles of the Declaration of Helsinki (1964). Written informed consent was obtained from all participants prior to sample collection. All animal experiments were approved by the Ethics Committee of Soochow University (No. SUDA20240711A09). All animal experiments were performed in accordance with a protocol approved by the Institutional Animal Care and Use Committee of Soochow University.

Conflicts of Interest: The authors declare no conflicts of interest to report regarding the present study.

Abbreviations

CLDN9	Claudin 9
FBS	Fetal Bovine Serum
TCGA	The Cancer Genome Atlas
PBS	Phosphate-Buffered Saline
qRT-PCR	Quantitative Real-Time Polymerase Chain Reaction

shRNA	Short hairpin RNA
CCK-8	Cell Counting Kit-8
DSS	Disease-Specific Survival
OS	Overall Survival
PFS	Progression-Free Survival
CI	Confidence Interval

References

1. Ramachandran R, Grantham T, Parvataneni S, Budh D, Gollapalli S, Reddy M, et al. Gastric cancer: clinical features, screening, diagnosis, treatment, and prevention. J Community Hosp Intern Med Perspect. 2024;14(2):49–57. doi:10.55729/2000-9666.1304.
2. Siegel RL, Giaquinto AN, Jemal A. Cancer statistics. CA Cancer J Clin. 2024;74(1):12–49. doi:10.3322/caac.21820.
3. Li J, Zhang H, Bei S, Zhang X, Li H, Ye L, et al. Disruption of Wnt/β-catenin pathway elevates the sensitivity of gastric cancer cells to PD-1 antibody. Curr Mol Pharmacol. 2022;15(3):557–69. doi:10.2174/1874467214666210617163821.
4. Zhang X, Jin M, Yao X, Liu J, Yang Y, Huang J, et al. Upregulation of LncRNA WT1-AS inhibits tumor growth and promotes autophagy in gastric cancer via suppression of PI3K/Akt/mTOR pathway. Curr Mol Pharmacol. 2024;17:e18761429318398. doi:10.2174/0118761429318398240918063450.
5. Li G, Li F, Wei N, Jia Q. Designing a risk prognosis model based on natural killer cell-linked genes to accurately evaluate the prognosis of gastric cancer. BIOCELL. 2023;47(9):2081–99. doi:10.32604/biocell.2023.029986.
6. Xu B, He P, Wang Y, Wang H, Zhang J, Zhu J, et al. PDT for gastric cancer—the view from China. Photodiagnosis Photodyn Ther. 2023;42(3):103366. doi:10.1016/j.pdpdt.2023.103366.
7. Machlowska J, Baj J, Sitarz M, Maciejewski R, Sitarz R. Gastric cancer: epidemiology, risk factors, classification, genomic characteristics and treatment strategies. Int J Mol Sci. 2020;21(11):4012. doi:10.3390/ijms21114012.
8. Sung H, Ferlay J, Siegel RL, Laversanne M, Soerjomataram I, Jemal A, et al. Global cancer statistics 2020: globocan estimates of incidence and mortality worldwide for 36 cancers in 185 countries. CA Cancer J Clin. 2021;71(3):209–49. doi:10.3322/caac.21660.
9. Li S, Yu W, Xie F, Luo H, Liu Z, Lv W, et al. Neoadjuvant therapy with immune checkpoint blockade, antiangiogenesis, and chemotherapy for locally advanced gastric cancer. Nat Commun. 2023;14(1):8. doi:10.1038/s41467-022-35431-x.
10. Christodoulidis G, Koumarelas KE, Kouliou MN. Revolutionizing gastric cancer treatment: the potential of immunotherapy. World J Gastroenterol. 2024;30(4):286–9. doi:10.3748/wjg.v30.i4.286.
11. Guan WL, He Y, Xu RH. Gastric cancer treatment: recent progress and future perspectives. J Hematol Oncol. 2023;16(1):57. doi:10.1186/s13045-023-01451-3.
12. Ilson DH. Advances in the treatment of gastric cancer: 2019. Curr Opin Gastroenterol. 2019;35(6):551–4. doi:10.1097/MOG.0000000000000577.
13. Matos TL, Souza PFN, de Moraes MEA, Rabenhorst SHB, Mesquita FP, Montenegro RC. Molecular characterization and biomarker discovery in gastric cancer progression through transcriptome meta-analysis. Comput Biol Med. 2024;183(1):109276. doi:10.1016/j.compbiomed.2024.109276.
14. Wu Z, Wang W, Zhang K, Fan M, Lin R. Epigenetic and tumor microenvironment for prognosis of patients with gastric cancer. Biomolecules. 2023;13(5):736. doi:10.3390/biom13050736.
15. Sugimoto K, Chiba H. The claudin-transcription factor signaling pathway. Tissue Barriers. 2021;9(3):1908109. doi:10.1080/21688370.2021.1908109.
16. Wang W, Zhou Y, Li W, Quan C, Li Y. Claudins and hepatocellular carcinoma. Biomed Pharmacother. 2024;171(3):116109. doi:10.1016/j.biopha.2023.116109.
17. Zhuang X, Martin TA, Ruge F, Zeng JJ, Li XA, Khan E, et al. Expression of claudin-9 (CLDN9) in breast cancer, the clinical significance in connection with its subcoat anchorage proteins ZO-1 and ZO-3 and impact on drug resistance. Biomedicines. 2023;11(12):3136. doi:10.3390/biomedicines11123136.

18. Yasen A, Tuoheti M, Tu B, Zhang C, Ding Y, Tang F, et al. The correlation among Claudin-9, Tyrosine kinase-2, and Signal transducers and activators of transcription-3 expressions in non-functioning pituitary adenoma and invasiveness. Neuro Endocrinol Lett. 2023;44(8):537–46.
19. Endo Y, Sugimoto K, Kobayashi M, Kobayashi Y, Kojima M, Furukawa S, et al. Claudin-9 is a novel prognostic biomarker for endometrial cancer. Int J Oncol. 2022;61(5):135. doi:10.3892/ijo.2022.5425.
20. Hong L, Wu Y, Feng J, Yu S, Li C, Wu Y, et al. Overexpression of the cell adhesion molecule claudin-9 is associated with invasion in pituitary oncocytomas. Hum Pathol. 2014;45(12):2423–9. doi:10.1016/j.humpath.2014.08.006.
21. Hu X, Ouyang W, Chen H, Liu Z, Lai Z, Yao H. Claudin-9 (CLDN9) promotes gastric cancer progression by enhancing the glycolysis pathway and facilitating PD-L1 lactylation to suppress CD8+ T cell anti-tumor immunity. Cancer Pathog Ther Forthcoming. 2024;74:229. doi:10.1016/j.cpt.2024.09.006.
22. Song J, Xu X, He S, Wang N, Bai Y, Chen Z, et al. Myristicin suppresses gastric cancer growth via targeting the EGFR/ERK signaling pathway. Curr Mol Pharmacol. 2023;16(7):712–24. doi:10.2174/1874467216666230103104600.
23. Hayashi D, Tamura A, Tanaka H, Yamazaki Y, Watanabe S, Suzuki K, et al. Deficiency of claudin-18 causes paracellular H^+ leakage, up-regulation of interleukin-1β, and atrophic gastritis in mice. Gastroenterology. 2012;142(2):292–304. doi:10.1053/j.gastro.2011.10.040.
24. Choi S, Kim N, Park JH, Nam RH, Song CH, Lee HS. Effect of *Helicobacter pylori* infection and its eradication on the expression of tight junction proteins in the gastric epithelium in relation to gastric carcinogenesis. Helicobacter. 2022;27(6):e12929. doi:10.1111/hel.12929.
25. Katoh M, Katoh M. Claudin 1, 4, 6 and 18 isoform 2 as targets for the treatment of cancer (Review). Int J Mol Med. 2024;54(5):100. doi:10.3892/ijmm.2024.5424.
26. Satake S, Semba S, Matsuda Y, Usami Y, Chiba H, Sawada N, et al. Cdx2 transcription factor regulates claudin-3 and claudin-4 expression during intestinal differentiation of gastric carcinoma. Pathol Int. 2008;58(3):156–63. doi:10.1111/j.1440-1827.2007.02204.x.
27. Wang C, Wang Y, Chen J, Wang Y, Pang C, Liang C, et al. CLDN18.2 expression and its impact on prognosis and the immune microenvironment in gastric cancer. BMC Gastroenterol. 2023;23(1):283. doi:10.1186/s12876-023-02924-y.
28. Jung H, Jun KH, Jung JH, Chin HM, Park WB. The expression of claudin-1, claudin-2, claudin-3, and claudin-4 in gastric cancer tissue. J Surg Res. 2011;167(2):e185–91. doi:10.1016/j.jss.2010.02.010.
29. Matsuda Y, Semba S, Ueda J, Fuku T, Hasuo T, Chiba H, et al. Gastric and intestinal claudin expression at the invasive front of gastric carcinoma. Cancer Sci. 2007;98(7):1014–9. doi:10.1111/j.1349-7006.2007.00490.x.
30. Zhang T, He Z, Liu Y, Jin L, Wang T. High expression of CLDN 18.2 is associated with poor disease-free survival of HER-2 positive gastric cancer. Int J Gen Med. 2024;17:1695–705. doi:10.2147/IJGM.S453883.
31. Ouban A, Ahmed AA. Claudins in human cancer: a review. Histol Histopathol. 2010;25(1):83–90. doi:10.14670/HH-25.83.
32. Liu H, Wang M, Liang N, Guan L. Claudin-9 enhances the metastatic potential of hepatocytes via Tyk2/Stat3 signaling. Turk J Gastroenterol. 2019;30(8):722–31. doi:10.5152/tjg.2019.18513.
33. Sharma RK, Chheda ZS, Das Purkayastha BP, Gomez-Gutierrez JG, Jala VR, Haribabu B. A spontaneous metastasis model reveals the significance of claudin-9 overexpression in lung cancer metastasis. Clin Exp Metastasis. 2016;33(3):263–75. doi:10.1007/s10585-015-9776-4.
34. Du Q, Lin Y, Ding C, Wu L, Xu Y, Feng Q. Pharmacological activity of matrine in inhibiting colon cancer cells VM formation, proliferation, and invasion by downregulating claudin-9 mediated EMT process and MAPK signaling pathway. Drug Des Devel Ther. 2023;17:2787–804. doi:10.2147/DDDT.S417077.
35. Wang ZH, Zhang YZ, Wang YS, Ma XX. Identification of novel cell glycolysis related gene signature predicting survival in patients with endometrial cancer. Cancer Cell Int. 2019;19(1):296. doi:10.1186/s12935-019-1001-0.